15 August 1997

ELSEVIER

Chemical Physics Letters 274 (1997) 411–421

CHEMICAL PHYSICS LETTERS

Low-lying electronic states and molecular structure of FeO_2 and FeO_2^-

Zexing Cao [a], Miquel Duran [b], Miquel Solà [b,*]

[a] *Department of Chemistry, Hunan Normal University, Changsha 410081 and Department of Chemistry, Xiamen University, Xiamen 361005, PR China*

[b] *Institute of Computational Chemistry and Department of Chemistry, Universitat de Girona, 17071 Girona, Catalonia, Spain*

Received 6 June 1996

Abstract

An ab initio theoretical study on the structures, molecular bonding and harmonic vibrational frequencies of the low-lying electronic states of FeO_2 and FeO_2^- has been carried out at the HF, MP2 and CCSD(T) levels of theory with the MIDI * and TZV * basis sets. For FeO_2, the properties of the ground state strongly depend on the level of the calculation. At the UHF level, the inserted linear dioxide $^3B_1$ state (C_{2v} subgroup notation) in $D_{\infty h}$ symmetry is found to be the most stable state. The inclusion of correlation energy by means of the MP2 and CCSD(T) methods results in an inserted dioxide $^1A_1$ state in C_{2v} symmetry as the lowest energy state. For FeO_2^-, the inserted linear dioxide $^6A_{2g}$ state (in D_{4h} subgroup notation) is the ground state at the HF, MP2 and CCSD(T) levels of theory with the TZV * basis set. Other stable and first order saddle points with possible side-on, end-on and inserted structures have been located on the potential energy hypersurfaces of FeO_2 and FeO_2^-. © 1997 Elsevier Science B.V.

1. Introduction

Transition metals, especially iron, play an essential role in the activation, transportation and storage of molecular oxygen [1,2]. A study of the interaction of Fe with oxygen is important for understanding such diverse processes as the corrosion of structural metals and oxygen transport in biological systems. The interactions of an Fe atom with oxygen (O_2) and superoxide (O_2^-) lead to the FeO_2 and FeO_2^- species which are basic molecular iron–oxygen systems.

The isomers of FeO_2 and FeO_2^- can take the following five possible structures (see Fig. 1): side-on adduct $Fe(O_2)$ (I), end-on adduct FeOO in $C_{\infty v}$ (II) and C_s symmetry (III) and inserted dioxide OFeO in C_{2v} symmetry (IV) and $D_{\infty h}$ symmetry (V).

From a theoretical point of view, these two iron–oxygen systems have been examined using different methods. Semi-empirical calculations [3] suggest the linear end-on $^3A''$ FeO_2 system to be the most stable isomer, while the linear inserted dioxide $^6A_1$ is found to be the most favored isomer for the FeO_2^- anion. HF/STO-3G * results [4] indicate that the most stable FeO_2 isomer is the $^7A_1$ inserted dioxide in C_{2v} symmetry, although only a few number of electronic states were analyzed in this study. Density functional

* Corresponding author.

PII S0009-2614(97)00686-6

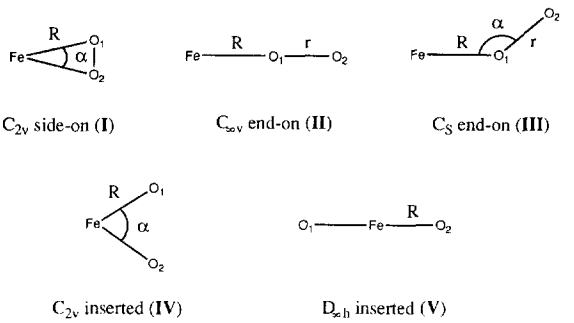

Fig. 1. Schematic drawing with labels for the geometrical parameters of the different FeO_2 isomers.

(DFT) calculations by Lyne et al. [5] on several singlet and triplet electronic states of FeO_2 indicated that the $^3B_2$ inserted dioxide form was the ground state, while recent DFT calculations by Chertihin et al. [6] on several triplet and quintet FeO_2 products yielded the $^3B_1$ inserted dioxide OFeO in C_{2v} symmetry as the most stable isomer. Finally, a recent ab initio investigation on the FeC_2 and FeC_2^- species found that the $^7A_2$ and $^6B_2$ electronic states in a C_{2v} side-on structure were the most stable at the HF and CISD levels of theory [7].

From an experimental point of view, the reactions between atomic Fe + O_2 and O_2^- have been examined in several works [8–13]. A matrix-isolation spectra indicated that the side-on structure was the most stable for FeO_2 [9]. Also, the aforementioned DFT study by Chertihin et al. [6] was complemented by matrix infrared spectra of the products of the reaction between laser-ablated iron atoms and molecular oxygen in argon. Sharp infrared absorptions at 1204.5, 945.8 and 797.1, and 956.0 cm^{-1} were identified as the $^3A''$ end-on FeOO, $^3B_1$ inserted C_{2v} OFeO and $^5A_1$ side-on C_{2v} Fe(O_2) electronic states, respectively. Finally, a recent photoelectron spectroscopy study suggested that FeO_2 and FeO_2^- have a similar structure and that there is a small bond angle change from the anion to the neutral FeO_2 [13]. Further, the strong intensity seems to demonstrate that the neutral and ion states differ by only one spin orbital. The electron affinity (EA) of FeO_2 found in this work was 2.358 eV. The study concluded that, since both Fe and O_2 have low EAs, this high EA is inconsistent with either a side-on Fe(O_2) adduct or a linear or bent end-on FeOO structure.

Despite their relevance, none of these studies reported conclusive data on the electronic structure and geometry of the ground states of the FeO_2 and FeO_2^- systems. Further, the FeO_2^- system has not yet been analyzed with ab initio methods. Thus, the aim of this Letter is to perform an ab initio theoretical analysis on the ground and low-lying electronic excited states of these two iron–oxygen systems. The study includes the electronic structures, geometries, molecular bonding and harmonic vibrational frequencies of the FeO_2 and FeO_2^- species.

2. Method of calculation

The basis set employed in this study was the Huzinaga split-valence basis set [14] augmented with two polarization functions denoted as MIDI*. The most stable systems were also studied using a triple zeta valence basis set augmented with polarization functions (TZV*) [15,16]. All the calculations were done within the unrestricted Hartree–Fock method (UHF) except singlets which were calculated within the restricted Hartree–Fock formalism. It is not trivial to obtain an initial guess with good convergence for these systems. Initial guesses of the electron configurations for the low-lying states in our calculations, were constructed by proper UHF SCF molecular orbitals obtained from different SCF convergence methods at several trial geometries. For some electronic states it was necessary to consider a different symmetry for the single Slater determinant and the nuclear framework [17,18]. In this case, proper subgroups were used in the calculation. Optimization of geometries was done by an SCF energy gradient method, and the vibrational frequencies for stationary points on the potential energy surfaces (PES) were computed numerically. The symmetries of the vibrational modes were identified from an analysis of the vibrational vectors. Correlation energies were estimated through the second-order Møller–Plesset perturbation (MP2) method at the HF geometries. The most relevant electronic states were also examined by means of coupled cluster calculations which included single and double excitations with a noniterative inclusion of the triple excitations (CCSDT(T)) [19] at the HF geometries. Finally, in order to test whether the HF optimized geometries

Table 1
Electronic configurations, optimized geometries and harmonic vibrational frequencies of the low-lying electronic states of FeO_2 and FeO_2^- obtained with the MIDI* basis set

State	Configuration [a]	Geometry [b]	Frequencies [c]
neutral FeO_2			
side-on in C_{2v} symmetry (I)			
$^7A_1$	$3a_1^2\ 2b_1^2\ b_2^2\ a_2^2$	$R = 1.993$	211.6 (0.04, b_2), 490.3 (1.83, a_1)
	$3a_1\ b_1\ b_2\ a_2$	$\alpha = 38.0$	1456.1 (0.00, a_1)
A^5A_2	$4a_1^2\ 2b_1^2\ b_2^2\ a_2^2$	$R = 2.008$	146.3 (2.07, b_2), 482.9 (74.9, a_1)
	$2a_1\ b_1\ b_2$	$\alpha = 37.7$	1436.9 (0.04, a_1)
$B\ ^5A_2$	$5a_1^2\ 2b_1^2\ b_2^2$	$R = 1.994$	60.4i (0.00, b_2), 506.2 (1.58, a_1)
	$2a_2\ b_1\ b_2$	$\alpha = 38.0$	1452.0 (0.0, a_1)
A^5A_1	$4a_1^2\ b_1^2\ 2b_2^2\ a_2^2$	$R = 1.984$	69.4 (0.26, b_2), 501.5 (1.47, a_1)
	$a_1\ b_1\ b_2\ a_2$	$\alpha = 38.2$	1436.1 (0.00, a_1)
$B\ ^5A_1$	$4a_1^2\ 2b_1^2\ b_2^2\ a_2^2$	$R = 1.784$	857.9 (41.3, b_2), 658.1 (2.28, a_1)
	$a_1\ b_1\ b_2\ a_2$	$\alpha = 50.4$	940.4 (1.42, a_1)
$^3B_2$	$4a_1^2\ 2b_1^2\ b_2^2\ 2a_2^2$	$R = 2.004$	397.0i (0.12, b_2), 431.0 (1.16, a_1)
	$a_1\ b_2$	$\alpha = 38.4$	1377.2 (0.29, a_1)
$A\ ^1A_1$	$5a_1^2\ 2b_1^2\ 2b_2^2\ a_2^2$	$R = 1.708$	734.9 (0.96, b_2), 820.9 (1.28, a_1)
		$\alpha = 49.6$	1039.0 (2.39, a_1)
$B\ ^1A_1$	$4a_1^2\ 2b_1^2\ 2b_2^2\ 2a_2^2$	$R = 1.750$	683.0 (0.85, b_2), 777.6 (1.37, a_1)
		$\alpha = 49.6$	1021.8 (0.66, a_1)
end-on in $C_{\infty v}$ symmetry (II)			
$^7A_2$ [d]	$3a_1^2\ 4e^2$	$R = 1.701$	280.1 (0.15, π), 575.7 (5.11, σ)
	$2a_1\ b_1\ b_2\ 2e$	$r = 1.220$	1361.31 (68.77, σ)
$^5B_1$ [e]	$5a_1^2\ 2b_2^2\ b_1^2$	$R = 1.788$	177.3i (0.16, π), 129.7i (0.10, π)
	$2a_1\ b_1\ a_2$	$r = 1.299$	540.0 (1.22, σ), 1388.1 (4.78, σ)
$^1A_1$ [d]	$4a_1^2\ 4e^2\ b_2^2\ b_1^2$	$R = 1.555$	163.0i (1.81, π), 467.8 (0.09, σ)
		$r = 1.410$	1211.5 (6.52, σ)
end-on in C_s symmetry (III)			
$^3A''$	$6a'^2\ 3a''^2$	$R = 1.838$	122.4 (0.02, a'), 612.1 (1.42, a')
	$a'\ a''$	$\alpha = 110.4\ r = 1.329$	1238.9 (1.62, a')
$^3A'$	$6a'^2\ 3a''^2$	$R = 1.837$	142.8 (0.02, a'), 577.1 (1.91, a')
	$2a'$	$\alpha = 123.9\ r = 1.315$	1285.4 (2.53, a')
inserted dioxide in C_{2v} symmetry (IV)			
$^3B_2$	$4a_1^2\ 3b_1^2\ b_2^2\ a_2^2$	$R = 1.886$	463.7 (2.58, b_2), 103.4 (0.02, a_1)
	$a_1\ b_2$	$\alpha = 127.7$	405.2 (0.60, a_1)
$^1A_1$	$4a_1^2\ 3b_2^2\ 2b_1^2\ a_2^2$	$R = 1.500$	1266.2 (15.18, b_2), 94.9 (2.45, a_1)
		$\alpha = 169.8$	1275.2 (0.34, a_1)
inserted dioxide in $D_{\infty h}$ symmetry (V)			
$^7B_{3u}$ [f]	$2a_g^2\ 2b_{1u}^2\ b_{3g}^2\ b_{2g}^2\ b_{3u}^2$	$R = 1.790$	111.0 (1.67, π), 215.0 (1.59, π)
	$2a_g\ b_{2g}\ b_{1g}\ b_{3g}\ b_{3u}$		625.6 (0.0, σ_g), 750.8 (2.22, σ_u)
$^7A_{1u}$ [g]	$2a_{1g}^2\ a_{2u}^2\ 2e_g^2\ 2e_u^2$	$R = 1.703$	543.1 (0.17, π), 706.2 (0.00, σ_g)
	$a_{1g}\ a_{2u}\ b_{2g}\ b_{1g}\ e_g\ e_g$		830.4 (2.09, σ_u)
$^7B_2$ [e]	$3a_1^2\ 2b_2^2\ a_2^2\ b_1^2$	$R = 1.841$	117.9 (1.70, π), 122.9 (1.83, π)
	$2a_1\ 2b_2\ a_2\ b_1$		621.4 (0.00, σ_g), 760.2 (2.99, σ_u)
$^5B_{2g}$ [g]	$2a_{1g}^2\ 2a_{2u}^2\ 2e_g^2\ 2e_u^2$	$R = 1.742$	291.9 (19.7, π), 309.6 (29.8, π)
	$a_{1g}\ b_{2g}\ e_g\ e_g$		631.1 (0.00, σ_g), 782.9 (13.0, σ_u)
$^3B_{2g}$ [g]	$2a_{1g}^2\ 2a_{2u}^2\ 2e_g^2\ 2e_u^2\ b_{1g}^2$	$R = 1.745$	65.8 (2.42, π),
	$a_{1g}\ b_{2g}$		599.2 (33.8, σ_u), 620.5 (0.08, σ_g)
$^3B_2$ [h]	$3a_1^2\ 3b_1^2\ 2a_2^2\ b_1^2$	$R = 1.838$	91.7 (1.83, π), 187.4 (1.41, π)
	$a_1\ b_2$		586.7 (0.00, σ_g), 722.9 (2.27, σ_u)
$^3B_1$ [h]	$4a_1^2\ 3b_1^2\ a_2^2\ b_2^2$	$R = 1.802$	137.0 (1.80, π), 137.5 (1.54, π)
	$a_2\ b_2$		619.4 (0.00, σ_g), 756.0 (2.65, σ_u)

Table 1 (continued)

State	Configuration [a]	Geometry [b]	Frequencies [c]
$^1A_{1g}$ [g]	$2a_{1g}^2\ 2a_{2u}^2\ 2e_g^2\ 2e_u^2$	$R = 1.501$	59.4i (2.53, π)
	$b_{1g}^2\ b_{2g}^2$		1266.0 (15.15, σ_u), 1277.4 (0.18, σ_g)
FeO_2^- anion			
side-on C_{2v} symmetry (I)			
$^6A_1$	$4a_1^2\ 2b_1^2\ b_2^2\ a_2^2$	$R = 1.852$	533.4 (0.32, b_2), 596.4 (1.16, a_1)
	$2a_1\ b_1\ b_2\ a_2$	$\alpha = 47.5$	943.5 (0.99, a_1)
$^4A_2$	$5a_1^2\ 2b_1^2\ b_2^2\ a_2^2$	$R = 2.118$	147.8i (0.01, b_2), 369.4 (1.32, a_1)
	$a_1\ b_1\ b_2$	$\alpha = 35.6$	1474.8 (0.00, a_1)
$^4B_1$	$4a_1^2\ 2b_1^2\ 2b_2^2\ a_2^2$	$R = 1.851$	606.4 (0.02, b_2), 607.1 (1.36, a_1)
	$a_1\ a_2\ b_2$	$\alpha = 47.8$	943.9 (0.48, a_1) [d]
$^4B_2$	$4a_1^2\ 2b_1^2\ 2b_2^2\ a_2^2$	$R = 1.851$	603.4 (0.02, b_2), 606.2 (1.34, a_1)
	$a_1\ a_2\ b_1$	$\alpha = 47.8$	947.4 (0.48, a_1)
$^4A_1$	$5a_1^2\ 2b_1^2\ b_2^2\ a_2^2$	$R = 1.855$	487.3 (0.02, b_2), 610.8 (1.59, a_1)
	$a_2\ b_1\ b_2$	$\alpha = 47.7$	953.0 (0.40, a_1)
end-on in $C_{\infty v}$ symmetry (II)			
$^6B_2$ [e]	$5a_1^2\ 2b_1^2\ b_2^2$	$R = 1.890$	165.0i (0.0, π), 106.7i (0.0, π)
	$a_1\ b_1\ 2b_2\ a_2$	$r = 1.292$	412.2 (1.57, σ), 1355.1 (4.29, σ)
$^4B_2$ [d]	$4a_1^2\ b_1^2\ 4e^2$	$R = 1.699$	179.3i (0.01, π)
	$2e\ b_2$	$r = 1.458$	498.7 (0.06, σ), 983.6 (2.44, σ)
$^2A_1$ [d]	$4a_1^2\ b_1^2\ b_2^2\ 4e^2$	$R = 1.619$	195.4i (0.14, π)
	a_1	$r = 1.419$	526.4 (0.46, σ), 1156.6 (2.86, σ)
end-on in C_s symmetry (III)			
$^4A''$	$7a'^2\ 2a''^2$	$R = 2.3302$	141.1 (0.10, a'), 431.8 (1.25, a')
	$2a'\ a''$	$\alpha = 87.1\ r = 1.304$	1296.9 (0.75, a')
$^4A'$	$7a'^2\ 2a''^2$	$R = 2.845$	153.3 (0.03, a'), 452.1 (1.40, a')
	$a'\ 2a''$	$\alpha = 121.4\ r = 1.314$	1267.0 (2.10, a')
$^6A'$	$6a'^2\ 2a''^2$	$R_1 = 2.125$	56.9 (0.21, a'), 376.6 (1.25, a')
	$3a'\ 2a''$	$\alpha = 74.1\ r = 1.295$	1452.8 (0.05, a')
inserted dioxide in C_{2v} symmetry (IV)			
$^2A_1$	$4a_1^2\ 3b_2^2\ 2b_1^2\ a_2^2$	$R = 1.859$	153.8 (0.55, a_1), 514.5 (0.67, a_1)
	a_1	$\alpha = 117.3$	562.4 (0.65, b_2)
inserted dioxide in $D_{\infty h}$ symmetry (V)			
$^6A_2$ [d]	$4a_1^2\ 4e^2$	$R = 1.639$	105.8 (2.02, π)
	$a_1\ b_1\ b_2\ 2e$		1005.6 (0.02, σ), 1081.8 (4.84, σ)
$^4B_2$ [d]	$4a_1^2\ 4e^2\ b_1^2$	$R = 1.757$	566.6 (29.9, π)
	$b_2\ 2e$		560.4 (1.30, σ), 589.6 (0.03, σ)

[a] Core electrons are omitted. Numbers in front of molecular orbitals indicate the number of orbitals with the same symmetry in the wavefunction.
[b] R and r in Å and α in degrees.
[c] IR frequencies in cm^{-1} and intensities in debye^2 amu^{-1} Å^{-2}.
[d] C_{4v} symmetry notation.
[e] C_{2v} symmetry notation.
[f] D_{2h} symmetry notation.
[g] D_{4h} symmetry notation.
[h] Obtained with a C_{2v} initial geometry.

were consistent with the geometries obtained at higher levels of theory, some selected states were reoptimized using the quadratic configuration interaction method including single and double substitutions (QCISD) [20]. The programs used in this work were Gamess 95 [21] and Gaussian 94 [22].

3. Results and discussion

Equilibrium parameters, electronic configurations and harmonic vibrational frequencies of the low-lying states of FeO_2 and FeO_2^- obtained with the MIDI* basis set are listed in Table 1. Table 2 presents the total energies at the HF and MP2 levels of theory together with Mulliken charge populations. Results obtained with the TZV* basis set for selected electronic states are given in Tables 3 and 4.

3.1. The FeO_2 system

As far as FeO_2 is concerned, there are many states with energies close to the lowest energy. As a consequence, the computed ground state depends on the level of calculation. The inserted dioxide structure is found to be the most stable at all levels of theory, in agreement with recent experimental data [6,13] and previous theoretical studies [5,6]. However, the electronic state and the molecular structure (C_{2v} or $D_{\infty h}$) obtained for the ground state differ depending on the level of calculation.

For FeO_2, the C_{2v} inserted dioxide complex (IV) in the singlet $^1A_1$ state has the lowest MP2 and CCSD(T) energies, and should be the ground state of neutral FeO_2. The high stability of the dioxide structure was also seen in FeO_2^+ [23]. The high-intensity anti-symmetric stretching frequency of 1182.8 cm^{-1} obtained with the TZV* basis set is quite close to the experimentally observed frequency of 1204.5 cm^{-1} [6]. Nonetheless, isotopic substitution shows that this experimental frequency comes from an FeO_2 complex with two inequivalent oxygen atoms and thus can not be assigned to this C_{2v} inserted complex. In order to explain this experimental frequency it is more reasonable to assign this band to the end-on $^3A''$ or $^3A'$ states which have an almost pure O–O stretching with frequencies of 1224.1 and 1298.2 cm^{-1} (Table 3), respectively, both close to the experimental value. Chertihin et al. [6] have also assigned this experimental frequency to the $^3A''$ state based on B3LYP calculations which yielded a value 1159.8 cm^{-1} for the O–O stretching of this state. Our calculated $^3A'$ state is quite stable at the CCSD(T)//UHF level. Unfortunately, it has not been possible to converge the CCSD(T)//UHF calculation for the $^3A''$ state, but from the HF and MP2 values of these two states one may predict that the $^3A''$ state is lower in energy than the $^3A'$ state.

Among the inserted linear species, the $^1A_{1g}$ state has the lowest MP2 energy (Table 2). However, it is not a stable stationary point on the PES, since it has a degenerate bending mode with imaginary frequency. These linear $^1A_{1g}$ and C_{2v} $^1A_1$ states have the same charge distribution and nearly equal Fe–O separation, indicating a similar chemical bonding. In fact, the $^1A_{1g}$ state is the transition state between two $^1A_1$ states. For this reason it has not been analyzed further with the TZV* basis set. Indeed, the most stable inserted linear isomer is the triplet $^3B_1$ state, which was located by starting from a C_{2v} initial geometry. This state is disfavored with respect to the $^1A_1$ inserted dioxide state by only 2.28 kcal/mol at the CCSD(T)//UHF level. The UHF frequencies associated to this state do not correspond to any of the experimental frequencies reported [6].

In the inserted linear state $^7B_{3u}$ there is only one electron in the outer degenerate e_u orbitals (D_{4h} notation) and the symmetry of the single Slater determinant is different from that of the skeleton of the nuclei. For this symmetry broken state, the D_{2h} subgroup was used in the calculation. The results in Tables 1 and 3 for the $^7B_{3u}$ state show that the breaking of symmetry results in the loss of the degeneracy of the vibrational bending. This $^7B_{3u}$ state is related to the $^6A_{2g}$ state of FeO_2^- by the loss of a β electron in the degenerate e_u HOMO of the $^6A_{2g}$ state (vide infra).

For the side-on species of $Fe(O_2)$, the $^7A_1$ state has the lowest energy at all levels of theory employed. This state was found to be the ground state in a previous theoretical study [4]. Our results show that this state is 5.5 kcal/mol less stable than the $^1A_1$ state at the CCSD(T)//UHF level. For this state we have reoptimized the geometry at the QCISD level and we have obtained an Fe–O bond length of 2.001 Å and an ∠OFeO angle of 39.5 degrees. Since the UHF values are 2.045 Å and 36.9 degrees, this seems to indicate that already the UHF procedure yields a reasonable description of the geometry of the FeO_2 species. The $^7A_1$ state has an O–O bond length of 1.294 Å (1.353 Å at the QCISD level), larger than that of molecular oxygen (1.160 Å) and superoxide (1.267 Å). The spin populations on Fe and O are 5 and 0.5 respectively, which suggests that

Table 2
Total energies (in E_h) and charge distribution obtained with the MIDI* basis set at the HF optimized geometry

State	HF	MP2	Fe	O_1	O_2
neutral FeO_2					
side-on in C_{2v} symmetry (I)					
$^7A_1$	−1405.869304	−1406.297303	+0.68	−0.34	−0.34
$A\,^5A_2$	−1405.866991	−1406.296036	+0.68	−0.34	−0.34
$B\,^5A_2$	−1405.846783	−1406.274882	+0.68	−0.34	−0.34
$A\,^5A_1$	−1405.847654	−1406.275855	+0.68	−0.34	−0.34
$B\,^5A_1$	−1405.767334	−1406.250647	+1.14	−0.57	−0.57
$^3B_2$	−1405.827707	−1406.251248	+0.70	−0.35	−0.35
$A\,^1A_1$	−1405.597500	−1406.144787	+1.00	−0.50	−0.50
$B\,^1A_1$	−1405.622177	−1406.127012	+1.14	−0.57	−0.57
end-on in $C_{\infty v}$ symmetry (II)					
$^7A_2$	−1405.717409	−1406.248440	+0.51	−0.29	−0.22
$^5B_1$	−1405.826298	−1406.230264	+0.68	−0.63	−0.05
$^1A_1$	−1405.482270	−1406.025930	+1.02	−0.56	−0.46
end-on in C_s symmetry (III)					
$^3A''$	−1405.834276	−1406.241817	+0.68	−0.58	−0.10
$^3A'$	−1405.750465	−1406.164029	+0.69	−0.59	−0.10
inserted dioxide in C_{2v} symmetry (IV)					
$^1A_1$	−1405.593773	−1406.343328	+1.30	−0.65	−0.65
$^3B_2$	−1405.790538	−1406.165660	+0.50	−0.25	−0.25
inserted dioxide in $D_{\infty h}$ symmetry (V)					
$^7A_{3u}$	−1405.890055	−1406.267600	+1.26	−0.63	−0.63
$^7A_{1u}$	−1405.830124	−1406.235233	+1.24	−0.62	−0.62
$^7B_2$	−1405.889251	−1406.254731	+1.26	−0.63	−0.63
$^5B_{2g}$	−1405.602331	−1406.063418	+0.78	−0.39	−0.39
$^3B_{2g}$	−1405.799357	−1406.252344	+0.72	−0.36	−0.36
$^3B_2$	−1405.875593	−1406.243104	+1.23	−0.62	−0.62
$^3B_1$	−1405.905416	−1406.275588	+1.26	−0.63	−0.63
$^1A_{1g}$	−1405.593727	−1406.342809	+1.30	−0.65	−0.65
FeO_2^- anion					
side-on C_{2v} symmetry (I)					
$^6A_1$	−1405.833288	−1406.300998	+0.28	−0.64	−0.64
$^4A_2$	−1405.864437	−1406.303721	−0.28	−0.36	−0.36
$^4B_1$	−1405.805295	−1406.271930	+0.30	−0.65	−0.65
$^4B_2$	−1405.805299	−1406.272008	+0.30	−0.65	−0.65
$^4A_1$	−1405.812289	−1406.277402	+0.30	−0.65	−0.65
end-on in $C_{\infty v}$ symmetry (II)					
$^6B_2$	−1405.851423	−1406.271828	−0.25	−0.59	−0.16
$^4B_2$	−1405.745684	−1406.204248	+0.24	−0.71	−0.53
$^2A_1$	−1405.551013	−1406.053888	+0.21	−0.65	−0.56
end-on in C_s symmetry (III)					
$^4A''$	−1405.864944	−1406.297787	−0.27	−0.49	−0.24
$^4A'$	−1405.857496	−1406.278143	−0.25	−0.57	−0.18
$^6A'$	−1405.866056	−1406.304607	−0.27	−0.39	−0.34
inserted dioxide in C_{2v} symmetry (IV)					
$^2A_1$	−1405.756345	−1406.142233	+0.28	−0.64	−0.64

Table 2 (continued)

State	HF	MP2	Fe	O_1	O_2
inserted dioxide in $D_{\infty h}$ symmetry (V)					
$^6A_2$	−1405.838338	−1406.369545	+0.92	−0.96	−0.96
$^4B_2$	−1405.757980	−1406.195925	+0.44	−0.72	−0.72

a β electron on Fe is partially transferred to the antibonding π^* of O_2. The calculations show that the molecular orbitals contributing to the molecular bonding are mainly composed of 4s, 4p and 3d from Fe and bonding π and antibonding π^* from O_2. There is a partial charge transfer from the bonding π orbital of O_2 into the singly occupied symmetry-adapted orbitals of Fe, and much more backdonation of charge from the Fe into the π^* orbitals of oxygen (a good discussion in terms of molecular orbitals can be found in reference [5]). These two interactions weaken the O–O bond in coordinated O_2. As was found with the B3LYP methodology [6], this septet state is slightly below the $^5A_1$ state (5.5 kcal/mol at the CCSD(T)//UHF level). However, while the frequencies of the $^5A_1$ state (661.4 and 923.9 cm^{-1}) are quite close to the experimental frequencies of 548.4 and 956.0 cm^{-1}, the frequencies of the $^7A_1$ state do not match the experimental ones, and so these two experimentally observed frequencies have been assigned to the $^5A_1$ state.

For the end-on species of FeO_2, one linear $^7A_2$ and two C_s symmetry $^3A'$ and $^3A''$ stable states were located on the PES using the MIDI* basis set, but the linear $^7A_2$ state decayed to a Van der Waals complex with a large Fe–O distance of 4.463 Å during optimization using the TZV* basis set. Indeed, few end-on stable points were found, and usually the end-on species have lower stabilities than the side-on and inserted isomers. This can be understood by taking into account that in the end-on species the Fe interacts mainly with one oxygen atom of an O_2 molecule. In this case the dominant orbital contributing molecular bonding from O_2 is the lone pair electron orbital, which is lower in energy than the bonding π orbital and so less active for molecular bonding.

As a whole, if one considers the energetic values obtained at the CCSD(T)//UHF level, the inserted dioxide in the C_{2v} symmetry $^1A_1$ state must be considered to be the ground state for the FeO_2 system. The fact that the predicted 1182.8 cm^{-1} for this state has not been observed yet, does not rule out this assignment, since probably under experimental conditions only side-on and end-on FeO_2 complexes can be obtained. Further, inserted dioxide in $D_{\infty h}$ symmetry $^3B_1$, $^7B_{3u}$ and $^7B_2$ states are also found to be quite stable, and there is the possibility that the use of more accurate methodologies could change the relative stability order between these states. On the other hand, if one takes into account frequencies, only the calculated frequencies for the end-on in C_s symmetry $^3A''$ or $^3A'$ states and the side-on in C_{2v} symmetry $^5A_1$ state can explain some of the experimentally observed frequencies [6].

3.2. The FeO_2^- system

With respect to FeO_2^-, the results obtained with the TZV* basis set show that the inserted linear $^6A_{2g}$ state is the most stable at all levels of theory employed. At the CCSD(T)/TZV*//QCISD/TZV* level the difference between the inserted linear $^6A_{2g}$ and the side-on $^6A_1$ states is 60.4 kcal/mol, while at the CCSD(T)/TZV*//UHF/TZV* level the difference is 62.0 kcal/mol. Recent experimental data [13] agree with a linear or bent inserted structure for FeO_2^-. Our calculations show that the linear inserted $^6A_{2g}$ state is a stable stationary point on the PES. Any attempt to optimize a sextet inserted bent C_{2v} structure has always led to the $^6A_{2g}$ linear structure. The optimized Fe–O bond length for the $^6A_{2g}$ state is 1.714 Å at the UHF/TZV* level (Table 3) and 1.737 Å at the QCISD/TZV* level. As usual, the inclusion of correlation energy leads to a somewhat larger Fe–O bond length. However, this minor effect demonstrates that already the UHF procedure yields a reasonable description of the geometry of the FeO_2^- species.

On the other hand, for side-on isomers, the $^6A_1$ state has the lowest energy, the spin populations on

Table 3
Electronic configurations, optimized geometries and harmonic vibrational frequencies of the low-lying electronic states of FeO_2 and FeO_2^- obtained with the TZV * basis set

State	Configuration [a]	Geometry [b]	Frequencies [c]
neutral FeO_2			
side-on in C_{2v} symmetry (I)			
$^7A_1$	$3a_1^2\ 2b_1^2\ b_2^2\ a_2^2$	$R = 2.045$	206.5 (0.03, b_2), 456.9 (2.18, a_1)
	$3a_1\ b_1\ b_2\ a_2$	$\alpha = 36.9$	1414.8 (0.03, a_1)
$^5A_1$	$4a_1^2\ 2b_1^2\ b_2^2\ a_2^2$	$R = 1.831$	568.7 (0.00, b_2), 661.4 (2.28, a_1)
	$a_1\ b_1\ b_2\ a_2$	$\alpha = 48.2$	923.9 (1.15, a_1)
$^3B_2$	$4a_1^2\ 3b_1^2\ b_2^2\ a_2^2$	$R = 2.065$	486.5 (6.63, b_2), 231.9 (0.41, a_1)
	$a_1\ b_2$	$\alpha = 69.8$	449.2 (0.42, a_1)
end-on in $C_{\infty v}$ symmetry (II)			
$^7A_2$ [d]	$3a_1^2\ 4e^2$	$R = 4.463$	17.0 (0.00, π), 16.2 (0.00, σ)
	$2a_1\ b_1\ b_2\ 2e$	$r = 1.160$	1958.0 (0.00, σ)
end-on in C_s symmetry (III)			
$^3A''$	$6a'^2\ 3a''^2$	$R = 1.951$	162.9 (1.21, a'), 508.1 (1.22, a')
	$a'\ a''$	$\alpha = 106.1\ r = 1.318$	1224.1 (1.50, a')
$^3A'$	$6a'^2\ 3a''^2$	$R = 1.893$	142.7 (0.04, a'), 542.4 (2.07, a')
	$2a'$	$\alpha = 133.9\ r = 1.306$	1298.2 (3.37, a')
inserted dioxide in C_{2v} symmetry (IV)			
$^1A_1$	$4a_1^2\ 3b_2^2\ 2b_1^2\ a_2^2$	$R = 1.520$	1182.8 (24.2, b_2), 173.5 (2.17, a_1)
		$\alpha = 162.3$	1170.7 (0.24, a_1)
inserted dioxide in $D_{\infty h}$ symmetry (V)			
$^7B_{3u}$ [e]	$2a_g^2\ 2b_{1u}^2\ b_{3g}^2\ b_{2g}^2\ b_{3u}^2$	$R = 1.864$	116.0 (1.91, π), 190.3 (1.71, π)
	$2a_g\ b_{2g}\ b_{3g}\ b_{1g}\ b_{3u}$		560.4 (0.00, σ_g), 688.5 (2.92, σ_u)
$^7A_{1u}$ [f]	$2a_{1g}^2\ a_{2u}^2\ 2e_g^2\ 2e_u^2$	$R = 1.811$	46.3 (0.88, π), 690.8 (0.0, σ_g)
	$a_{1g}\ a_{2u}\ b_{2g}\ b_{1g}\ e_g\ e_g$		754.7 (1.52, σ_u)
$^7B_2$ [g]	$3a_1^2\ 2b_2^2\ a_2^2\ b_1^2$	$R = 1.905$	113.4 (1.97, π), 128.6 (1.81, π)
	$2a_1\ 2b_2\ a_2\ b_1$		574.5 (0.00, σ_g), 704.7 (3.89, σ_u)
$^3B_1$ [h]	$4a_1^2\ 3b_1^2\ a_2^2\ b_2^2$	$R = 1.873$	131.6 (1.87, π), 137.7 (1.67, π)
	$a_2\ b_2$		562.6 (0.00, σ_g), 694.9 (3.38, σ_u)
FeO_2^- anion			
side-on in C_{2v} symmetry (I)			
$^6A_1$	$4a_1^2\ 2b_1^2\ b_2^2\ a_2^2$	$R = 1.922$	474.6 (0.47, b_2), 579.9 (3.02, a_1)
	$2a_1\ b_1\ b_2\ a_2$	$\alpha = 45.5$	935.7 (0.70, a_1)
$^4A_2$	$4a_1^2\ 2b_1^2\ b_2^2$	$R = 1.938$	288.9 (0.27, b_2), 579.3 (2.73, a_1)
	$2a_2^2\ a_1\ b_1\ b_2$	$\alpha = 45.4$	930.1 (0.38, a_1)
$^4B_2$	$4a_1^2\ 2b_1^2\ 2b_2^2\ a_2^2$	$R = 1.927$	580.4 (0.25, b_2), 576.8 (2.97, a_1)
	$a_1\ b_1\ a_2$	$\alpha = 45.5$	922.6 (0.49, a_1)
end-on in C_s symmetry (III)			
$^4A''$	$6a'^2\ 3a''^2$	$R = 2.103$	135.4 (0.04, a'), 322.1 (0.78, a')
	$2a'\ a''$	$\alpha = 127.1\ r = 1.304$	1276.4 (2.54, a')
inserted dioxide in C_{2v} symmetry (IV)			
$^2A_1$	$4a_1^2\ 3b_2^2\ 2b_1^2\ a_2^2$	$R = 1.985$	491.8 (9.72, b_2), 153.8 (0.91, a_1)
	a_1	$\alpha = 110.8$	466.1 (1.88, a_1)
inserted dioxide in $D_{\infty h}$ symmetry (V)			
$^6A_{2g}$ [f]	$2a_{1g}^2\ 2a_{2u}^2\ 2e_g^2\ 2e_u^2$	$R = 1.714$	146.3 (0.88, π), 837.5 (0.0, σ_g)
	$a_{1g}\ b_{2g}\ b_{1g}\ e_g\ e_g$		965.4 (12.6, σ_u)

Table 3 (continued)

State	Configuration [a]	Geometry [b]	Frequencies [c]
O_2 and O_2^-			
$^3B_2$ [g]	$4a_1^2\ 2b_1^2\ b_2^2$ $b_1\ a_2$	$r = 1.160$	1940.3
$^2B_1$ [g]	$4a_1^2\ 2b_1^2\ b_2^2\ a_2^2$ b_1	$r = 1.297$	1395.5

[a] Core electrons are omitted. Numbers in front of molecular orbitals indicate the number of orbitals with the same symmetry in the wavefunction.
[b] R and r in Å and α in degrees.
[c] IR frequencies in cm^{-1} and intensities in debye^2 amu^{-1} Å^{-2}.
[d] C_{4v} symmetry notation.
[e] D_{2h} symmetry notation.
[f] D_{4h} symmetry notation.
[g] C_{2v} symmetry notation.
[h] Obtained with a C_{2v} initial geometry.

Table 4
Total energies (in E_h) and charge distribution obtained with TZV* basis set at the HF optimized geometry

State	HF	MP2	CCSD(T)	Fe	O_1	O_2
neutral FeO_2						
side-on in C_{2v} symmetry (I)						
$^7A_1$	−1412.108914	−1412.577186	−1412.609124	+0.60	−0.30	−0.30
$^5A_1$	−1412.023871	−1412.557837	−1412.600399	+1.08	−0.54	−0.54
$^3B_2$	−1412.053259	−1412.436617	−1412.535339	+0.50	−0.25	−0.25
end-on in $C_{\infty v}$ symmetry (II)						
$^7A_2$	−1411.999534	−1412.489390		+0.00	−0.00	−0.00
end-on in C_s symmetry (III)						
$^3A''$	−1412.003087	−1412.510280		+0.70	−0.51	−0.19
$^3A'$	−1411.992853	−1412.451105	−1412.600208	+0.65	−0.56	−0.09
inserted dioxide in C_{2v} symmetry (IV)						
$^1A_1$	−1411.813214	−1412.659001	−1412.617815	+1.06	−0.53	−0.53
inserted dioxide in $D_{\infty h}$ symmetry (V)						
$^7B_{3u}$	−1412.152614	−1412.577629		+1.12	−0.56	−0.56
$^7A_{1u}$	−1412.015462	−1412.464591		+1.12	−0.56	−0.56
$^7B_2$	−1412.158088	−1412.571751	−1412.612904	+1.14	−0.57	−0.57
$^3B_1$	−1412.170683	−1412.588259	−1412.614174	+1.12	−0.56	−0.56
FeO_2^- anion						
side-on in C_{2v} symmetry (I)						
$^6A_1$	−1412.097303	−1412.621859	−1412.659178	+0.34	−0.67	−0.67
$^4A_2$	−1412.066966	−1412.585423		+0.36	−0.68	−0.68
$^4B_2$	−1412.062434	−1412.585664		+0.34	−0.67	−0.67
end-on in C_s symmetry (III)						
$^4A''$	−1411.997185	−1412.518457		−0.18	−0.56	−0.26
inserted dioxide in C_{2v} symmetry (IV)						
$^2A_1$	−1412.020471	−1412.452577		+0.40	−0.70	−0.70
inserted dioxide in $D_{\infty h}$ symmetry (V)						
$^6A_{2g}$	−1412.154121	−1412.725951	−1412.757936	+1.00	−1.00	−1.00

Fe and O being 4.92 and 0.04, respectively. The $^6A_1$ state can be considered as an iron–oxygen molecular complex formed by bonding interactions similar to those found in side-on neutral $Fe(O_2)$ complexes. An activation of the O–O bond in coordinated O_2^-, similar to the one present for neutral $Fe(O_2)$, is observed for the side-on species of FeO_2^-. At the QCISD/TZV* level, the optimized Fe–O bond length for this state is 1.884 Å and the ∠OFeO angle is 48.3°, again this geometry being close to the optimized geometry found at the UHF/TZV* level (Table 3).

Based on Koopmans' theorem the ionization potential (IP), obtained from the UHF/TZV* HOMO energies, of the most stable linear $^6A_{2g}$ and side-on in C_{2v} symmetry $^6A_1$ states are 4.16 and 2.54 eV, respectively, the latter value being close to the recently reported experimental value of 2.358 eV [13]. Despite the experimentally side-on and end-on complexes being disregarded based on the low EAs of Fe and O_2 [13], our calculations show that this side-on C_{2v} symmetry $^6A_1$ state can explain the experimental IP of FeO_2^-. Furthermore, loss of the a_1 HOMO electron of the side-on in C_{2v} symmetry $^6A_1$ state of FeO_2^- yields the side-on in C_{2v} symmetry $^5A_1$ state of FeO_2. The CCSD(T)/TZV*//UHF/TZV* energy difference between these two states is 1.60 eV, which is somewhat lower than the experimental IP of FeO_2^-, as expected from the fact that the energy of the $^5A_1$ state has been computed allowing geometry relaxation. On the other hand, the CCSD(T)/TZV*//UHF/TZV* energy difference between the linear inserted dioxide $^6A_{2g}$ and $^7B_2$ states of FeO_2^- and FeO_2, respectively, is 3.95 eV, which is larger than the experimental value. The IPs computed from the optimized geometries are usually smaller than the experimental values, and therefore these results also give support to the conclusion that experiment [13] is not observing the lowest state of FeO_2^-.

Experimentally, the sharp feature of the FeO_2^- photoelectron spectrum (UPS) suggests that there is little geometry change from the FeO_2^- anion to the FeO_2 neutral complex, and that probably the anion and the neutral species differ by only one spin orbital [13]. A possible explanation of this UPS can be found if one considers the removal of an electron from a doubly occupied e_u orbital in the $^6A_{2g}$ state of FeO_2^- which may lead to the $^7B_{3u}$ or $^7B_2$ inserted linear FeO_2. In these two states the FeO_2 system has a similar geometry to that of the FeO_2^- anion in the $^6A_{2g}$ state. Another possibility that one could take into account to explain the experimental UPS consists of the removal of the electron from the a_1 HOMO of the $^2A_1$ inserted C_{2v} state leading to the inserted dioxide in the C_{2v} symmetry $^1A_1$ state of FeO_2. However this possibility has been disregarded since this $^2A_1$ state is 171.5 kcal/mol less stable than the $^6A_{2g}$ state at the MP2 level, and also because the differences in geometry between the $^2A_1$ and $^1A_1$ states of FeO_2^- and FeO_2 are quite important. Finally, the most likely possibility is that the electron is lost from the a_1 HOMO of the side-on in C_{2v} symmetry $^6A_1$ state of FeO_2^-, yielding the side-on in C_{2v} symmetry $^5A_1$ state of FeO_2. There are three points that reinforce this possibility. First, the molecular structure of these two states is similar (see Table 3). Second, as commented before, the $^5A_1$ state has been identified as one of the states present in the products of the reaction between laser-ablated iron atoms and molecular oxygen in argon [6]. Finally, based on the value of the calculated and experimental ionization potential of FeO_2^- it seems reasonable to believe that FeO_2^- was obtained in the $^6A_1$ state. This notwithstanding, our calculations support the inserted linear dioxide $^6A_{2g}$ state as the ground state of FeO_2^-.

Acknowledgements

This work has been supported by the Spanish DGICYT Project No. PB95-0762. We thank the Centre de Supercomputació de Catalunya (CESCA) for a generous allocation of computing time. ZC gratefully acknowledges the Institute of Computational Chemistry of the Universitat de Girona for a grant which made this work possible. The authors are indebted to the Referee for fruitful comments.

References

[1] (a) L.I. Simandi, Dioxygen Activation and Homogeneous Catalytic Oxidation; Elsevier, Amsterdam, 1991. (b) L.I. Simandi, Catalytic Activation of Dioxygen by Metal Complexes, Kluwer, Dordrecht, 1992.

[2] (a) N. Kitajima, Y. Moro-oka, J. Chem. Soc. Dalton Trans. (1993) 2665. (b) L. Shu, J.C. Nesheim, K. Kauffmann, E. Münck, J.D. Lipscomb, L. Que Jr., Science 275 (1997) 515.
[3] G. Blyholder, J. Head, F. Ruette, Inorg. Chem. 21 (1982) 1539.
[4] M. Helmer, J.M.C. Plane, J. Chem. Soc. Faraday Trans. 90 (1994) 395.
[5] P.D. Lyne, D.M.P. Mingos, T. Ziegler, A. Downs, Inorg. Chem. 32 (1993) 4785.
[6] (a) G.V. Chertihin, W. Saffel, J.T. Yustein, L. Andrews, M. Neurock, A. Ricca, C.W. Bauschlicher, J. Phys. Chem. 100 (1996) 5261. (b) L. Andrews, G.V. Chertihin, A. Ricca, C.W. Bauschlicher, J. Am. Chem. Soc. 118 (1996) 467.
[7] Z. Cao, J. Mol. Struct. (Theochem) 365 (1996) 211.
[8] S. Abramowitz, N. Acquista, I.W. Levin, Chem. Phys. Lett. 50 (1977) 423.
[9] S. Chang, G. Blyholder, J. Fernandez, Inorg. Chem. 20 (1981) 2813.
[10] (a) L.V. Serebrennikov, Vestn. Mosk. Univ. Ser. 2, Khim. 29 (1988) 451. (b) L.V. Serebrennikov, Sc. D. Thesis, Moscow State University, 1990, Moscow.
[11] R.L. Whetten, D.M. Cox, D.J. Trevor, A. Kaldor, J. Phys. Chem. 89 (1984) 566.
[12] S.A. Mitchell, P.A. Hackett, J. Chem. Phys. 93 (1990) 7822.
[13] J. Fan, L.S. Wang, J. Chem. Phys. 102 (1995) 8714.
[14] S. Huzinaga, J. Andzelm, M. Klobukowski, E. Radzio-Andzelm, Y. Sakai, H. Tatewaki, Gaussian Basis sets for Molecular Calculations, Elsevier, Amsterdam, 1984.
[15] T.H. Dunning, J. Chem. Phys. 55 (1971) 716.
[16] A.K. Rappe, T.A. Smedley, W.A. Goddard III, J. Phys. Chem. 85 (1981) 2607.
[17] C. Liang, H.F. Schaefer III, Chem. Phys. Lett. 169 (1990) 150.
[18] Z. Cao, J. Zhang, A. Tian, G. Yan, J. Mol. Struct. (Theochem) 333 (1995) 191.
[19] G.E. Scuseria, H.F. Schaefer III, J. Chem. Phys. 90 (1989) 3700.
[20] J.A. Pople, M. Head-Gordon, K. Raghavachari, J. Chem. Phys. 87 (1987) 5968.
[21] M.W. Schmidt, K.K. Baldridge, J.A. Boatz, S.T. Elbert, M.S. Gordon, J.H. Jensen, S. Koseki, N. Matsunaga, K.A. Nguyen, S.J. Su, T.L. Windus, M. Dupuis, J.A. Montgomery, J. Comput. Chem. 14 (1993) 1347.
[22] M.J. Frisch, G.W. Trucks, H.B. Schlegel, P.M.W. Gill, B.G. Johnson, M.A. Robb, J.R. Cheesman, T. Keith, G.A. Petersson, J.A. Montgomery, K. Raghavachari, M.A. Al-Laham, V.G. Zakrzewski, J.V. Ortiz, J.B. Foresman, C.Y. Peng, P.Y. Ayala, W. Chen, M.W. Wong, J.L. Andrés, E.S. Replogle, R. Gomerts, R.L. Martin, D.J. Fox, J.S. Binkley, D.J. DeFrees, J. Baker, J.J.P. Stewart, M. Head-Gordon, C. Gonzalez, and J.A. Pople, Gaussian 94, Revision A.1, Gaussian, Pittsburgh, PA, 1995.
[23] D. Schröder, A. Fiedler, J. Schwarz, H. Schwarz, Inorg. Chem. 33 (1994) 5094.